Int. J. Heat Mass Transfer. Vol. 16, pp. 1611–1627. Pergamon Press 1973. Printed in Great Britain

HEAT TRANSFER IN NUCLEATE BOILING, MAXIMUM HEAT FLUX AND TRANSITION BOILING

G. HESSE*

Institut für Thermodynamik, Technische Universität Berlin, Berlin, W. Germany

(*Received* 18 *October* 1972)

Abstract—Characteristic boiling curves of the refrigerants (Freon) R12, R113 and R114 were determined for pressures up to 30 bar. The test fluids boiled on the outsides of a smooth nickel tube and of a grooved tube.

By application of Stephan's stability condition stable operating points could be maintained at maximum heat flux density and in the transition region. Due to the differing slopes of the characteristic boiling curves the stability condition in the transition region is easier to fulfil at low pressures than at high pressures. By using a test tube with grooves it was possible to favourably influence the shape of the characteristic boiling curves with respect to heat transfer and stability.

NOMENCLATURE

D, bubble diameter at departure [m];
g, gravitational acceleration [m/s^2];
$h = \dot{q}/\Delta T$, heat-transfer coefficient [W/m^{2}K];
$\Delta h/h$, uncertainty in heat-transfer coefficient [%];
k, thermal conductivity [W/mK];
p, pressure [bar];
$\dot{q}$, heat flux density [W/m^2];
r, radius of tube [m];
R_W, thermal resistance [m^{2}K/W];
R_p, roughness (DIN 4762) [10^{-6}m];
s, wall thickness [m];
T, temperature [°C];
$\Delta T = T_W - T_L$, temperature difference [K];
w, flow velocity [m/s].

Greek letters

ρ, density [kg/m^3];
σ, surface tension [kg/s^2];
θ, wetting angle [deg].

Subscripts

1, inside;
2, outside;
cbc, characteristic boiling curve;
chs, characteristic of heating surface;
F, fluid;
L, liquid;
V, vapour;
W, wall.

* Present address: Dept. of Mechanical Engineering, 125 Mechanical Engineering Building, University of Minnesota, Minneapolis 55455 Minnesota, U.S.A.

1. INTRODUCTION

IN ORDER to avoid destruction or sudden changes from nucleate to film boiling evaporators are usually operated well below the maximum heat flux density. Irrespective of whether indirect fluid heating or direct electrical heating are used, it is possible to transfer heat at maximum heat flux density and in the transition region between nucleate and film boiling without a change of the boiling mechanisms as long as a certain stability condition is fulfilled that was first derived by Stephan [1, 2] and was later also established by other authors [3–5].

The studies that led to this stability condition showed that it is useful to know the shape of the $\dot{q}$, ΔT-characteristics in the transition region between nucleate and film boiling, since it is then easier to estimate how closely the maximum heat flux density may be approached in cases, with no stability in the transition region. Moreover, means may be devised to influence the boiling process in such a way that the peak of the $\dot{q},\Delta T$-curve broadens over a wider range of the temperature difference ΔT or that its slope is less precipitous in the transition region. By such means it is easier to achieve stable boiling conditions at maximum heat flux density and in the transition region. The aim of this investigation was therefore to determine for various test fluids the $\dot{q},\Delta T$-characteristics ranging from nucleate boiling to film boiling. Furthermore the investigation was to reveal the influence of different pressures and of various forms of surface geometry.

Contrary to the large number of test results for the range of nucleate and film boiling to be found in literature, there is only little experimental information concerning heat transfer in the transition region. Those results published were mostly gained at atmospheric pressure. In some cases the test apparatus only permitted measurements during unsteady operation [6, 7] or, due to stability problems, only few test results were obtained in the vicinity of the point of minimum heat flux density [3, 8].

2. STABILITY CONDITIONS FOR EVAPORATORS

To facilitate the understanding of the experimental technique used in this investigation it is advisable to first elaborate on the stability condition derived by Stephan [1, 2].

The thermodynamic system to be described in conjunction with boiling phenomena consists of the boiling liquid, the heated wall and in some cases the fluid used for heating. It was divided by Stephan into two sub-systems. Sub-system 1 consists of the boiling liquid and also comprises properties of the evaporator surface as far as they influence the boiling process (such as wettability or roughness). The steady-state behaviour of sub-system 1 during heat transfer is described by the $\dot{q},\Delta T$-curve, the so-called characteristic boiling curve, which shows the heat flux density $\dot{q}$ transferred from the heating surface to the boiling liquid as a function of the temperature difference $\Delta T = T_W - T_L$ between heated wall and boiling liquid. The shape of the characteristic boiling curve in the $\dot{q},\Delta T$-diagram is, as we know, similar for all boiling liquids. For sub-system 2 Stephan obtained, from the Fourier–Kirchhoff energy equation, a curve in the $\dot{q},\Delta T$-diagram, which is called the heating surface characteristic. The equation for the heating surface characteristic during steady-state operation is [1, 2]:

$$\dot{q} = -\frac{1}{R_W}.\Delta T + \frac{1}{R_W}(T_F - T_L) + \dot{q}_0. \quad (1)$$

Operating points of an evaporator are fixed by the points of intersection of the characteristic boiling curve and the characteristic of the heating surface. Stephan showed, however, that such an intersection only then defines a stable operating point, if at the respective point the gradient of the characteristic boiling curve is greater than the gradient of the heating surface characteristic. Thus the stability condition for stable operating points of an evaporator is as follows:

$$\frac{1}{R_W} > -\left(\frac{\mathrm{d}(\dot{q})}{\mathrm{d}(\Delta T)}\right)_{\mathrm{cbc}}. \quad (2)$$

If the heated wall is that of a tube, on the outside of which a liquid is boiling at a temperature T_L and along the inside of which there is a mass flow at the temperature T_F, the thermal resistance R_W is:

$$R_W = \frac{\dfrac{k_W}{h_F s} + \dfrac{r_1}{s}\ln\dfrac{r_2}{r_1}}{\dfrac{r_1}{r_2}}\frac{s}{k_W}. \quad (3)$$

Correspondingly, for heating through a plane wall we have:

$$R_W = \frac{1}{h_F} + \frac{s}{k_W}. \quad (3a)$$

The heat flux density $\dot{q}_0$ in equation (1) is a function of the thermal resistance R_W, of the sources of internal energy and of geometry. If one assumes that the physical properties do not change in the relevant temperature range, the characteristic of the heating surface represented by equation

(1) is a straight line with the gradient:

$$\left(\frac{d(\dot{q})}{d(\Delta T)}\right)_{chs} = -\frac{1}{R_W}. \quad (4)$$

Technical evaporators always have characteristics by which the stability condition in the region of nucleate and film boiling is fulfilled. In the region of transition boiling, however, it is usually necessary to take particular precautions to obtain stable boiling conditions. One such measure, according to Stephan, consists in leading a mass flow along that side of the heating wall that is not in contact with the boiling liquid. This mass flow can at the same time be used as heating medium for the boiling liquid or else, as for instance in case of direct electrical or nuclear heating of the wall, not contribute at all to the heat transfer, cf. Fig. 1. All intermediate states, where heating is partly effected by the mass flow and partly through heat sources in the wall, are also possible. Furthermore, it is possible to let both the boiling liquid and the mass flow absorb heat from the wall heated by heat sources. Thus, it can be generally said:

$$\dot{q}_F \gtreqless 0 \quad (5)$$

with $\dot{q}_F$ being the mean value as to time and place of the heat flux transferred by the mass flow.

The slope of the heating surface characteristic as the relevant parameter for stable working conditions is independent of whether the mass flow participates in the heat transfer or not. Only the heat-transfer coefficient h_F between the mass flow and the heated wall, the thermal conductivity k_W and the geometry of the wall determine the magnitude of the thermal resistance and thereby the slope of the steady-state characteristic of the heating surface.

The physical objective of the mass flow with its stabilizing effect on the boiling process becomes clear if one studies the transient behaviour of the system consisting of both the heated wall and the boiling liquid. As a particularly illustrative example we shall consider the case that the heat transferred to the boiling liquid is completely generated by internal energy sources (Fig. 1(b), $\dot{q}_F = 0$). The heat flux density $\dot{q}$ and the temperature difference ΔT as defined above represent only the local and time mean values of these quantities. In actual fact, however, fluctuations of the heat flux density and thus also fluctuations in the temperature difference occur due to the periodical formation and separation of vapour bubbles from the heated surface. These fluctuations have been verified experimentally by several investigators [9–11]. By choosing a mass flow with high specific heat capacity, a high heat-transfer coefficient and a high flow velocity along the heated wall, we

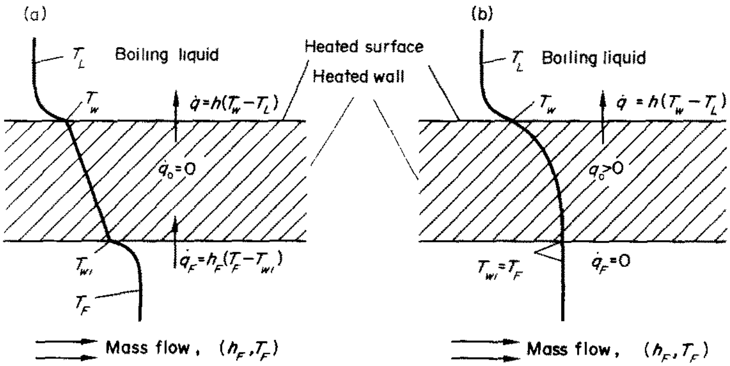

(a) Indirect heating by a mass flow

(b) Direct heating with heat sources in the wall and stabilization by a mass flow

FIG. 1. Heated wall.

achieve a compensation of such fluctuations. The deviations from the average heat flux value are absorbed or supplied by the mass flow without notable change in temperature. On the time average the mass flow does not transfer heat provided that its temperature exactly equals the local and time mean value of the temperature on the surface in contact with the mass flow.

This stabilization method is therefore equivalent to providing additional heat capacity for the heated wall. Consequently, any calculation of stability, as the above considerations show, has to take into account the transient behaviour of the system. If only the steady-state behaviour of the system is considered, there is no certainty that the real system behaves as predicted by the stability condition gained from a calculation for the steady-state system. Kovalev [3, 12], in his studies, did indeed obtain a correct result for the stability condition without, however, taking into account the transient behaviour of the entire system in the vicinity of a stable or unstable operating point [13]. According to Ouwerkerk [14] the stable or unstable behaviour during boiling is determined by heat conduction along the heated surface. This is inconsistent with the above statements, according to which the thermal resistance and the heat capacity are the governing parameters for stable behaviour. The method of measuring heat transfer in the regions of maximum heat flux density and transition boiling by direct electrical heating and simultaneous stabilization of the boiling process by a separate liquid has already been described by Poletavkin and coworkers [15] and was demonstrated with measurements at maximum heat flux density. However, the necessary stability condition, equation (2), was not observed by these authors.

3. OPERATING POINTS OF AN EVAPORATOR

Let us first study the point of maximum heat flux density (point 1 in Fig. 2) as an operating point of an evaporator and consider the effect of various possible shapes of the heating surface characteristic. We shall assume that the physical properties are independent of temperature so that the characteristics of the heating surface are straight lines. This restriction, although not principally necessary, will simplify the following discussion.

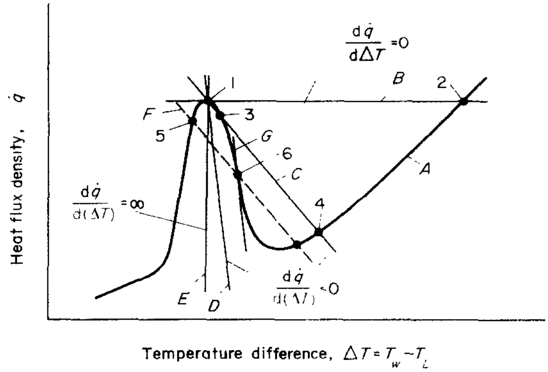

FIG. 2. Operating points.

In the case of direct heating without additional measures for the stabilization of the boiling process, the characteristic of the heating surface is a horizontal line (line *B* in Fig. 2). Accordingly, it has a gradient exactly equal to that of the characteristic boiling curve (*A*) at its maximum in point 1. According to the stability condition this is an indifferent operating point at which a minor disturbance of the equilibrium results in a change of the boiling condition to the region of film boiling, i.e. to the stable operating point 2. If, however, an evaporator with direct heating is stabilized by a mass flow or, if the evaporator is heated by a mass flow only, we have heating surface characteristics (*C*, *D*) that become increasingly steeper the greater the heat transfer coefficient h_F on the heated side of the wall and the smaller the thermal resistance s/k_W of this wall. The vertical characteristic of a heating surface (*E*) is a limiting case which is not attainable.

From the foregoing presentation we infer that an evaporator can be operated at maximum heat flux density without running the risk of the boiling condition changing over to the region of film boiling if one succeeds in making its heating surface characteristic (D) so precipitous that there is only one point of intersection (1) with the boiling curve (A). Such an intersection always characterizes a stable operating point, independent of whether there is direct or indirect heating. If there are further points of intersection (3, 4) of which the one in the transition region between nucleate and film boiling always represents an instable operating point (3), it is possible to obtain a new operating point (5) by a slight reduction of the heat flux density, i.e. by a parallel shift of heating surface characteristic towards nucleate boiling (F). This operating point then lies only slightly below the point of maximum heat flux density where minor disturbances of the equilibrium, however, now do not result in a change of the boiling mechanism. One can furthermore deduce from the discussion above that, independent of the kind of heating, stable boiling conditions in the transition region are only possible if the two characteristics (A, G) have only a single point of intersection (6). This is inconsistent with the frequently held opinion that generally all points of the characteristic boiling curve can be maintained in steady-state operation if the evaporator is heated by condensing steam or by a flowing fluid.

4. EXPERIMENTAL EQUIPMENT

The experimental equipment is shown simplified in Fig. 3. Further details are described in [16]. The test fluid boils on the outside of a tube in a boiling vessel. The vapour subsequently condenses in the condenser and the condensate flows back to the boiling vessel. The test tube may be heated in two ways. Either directly by an electrical current, or indirectly by a liquid (water) flowing inside the test tube. Both kinds of heating can also be combined. In order to obtain stable boiling conditions in the transition region the slope of the heating surface characteristic of the test section may be altered by increasing or reducing the flow velocity of the liquid within the tube and thereby also the heat transfer coefficient h_F. The highest flow velocity during measurements was 20 m/s. The test fluids were

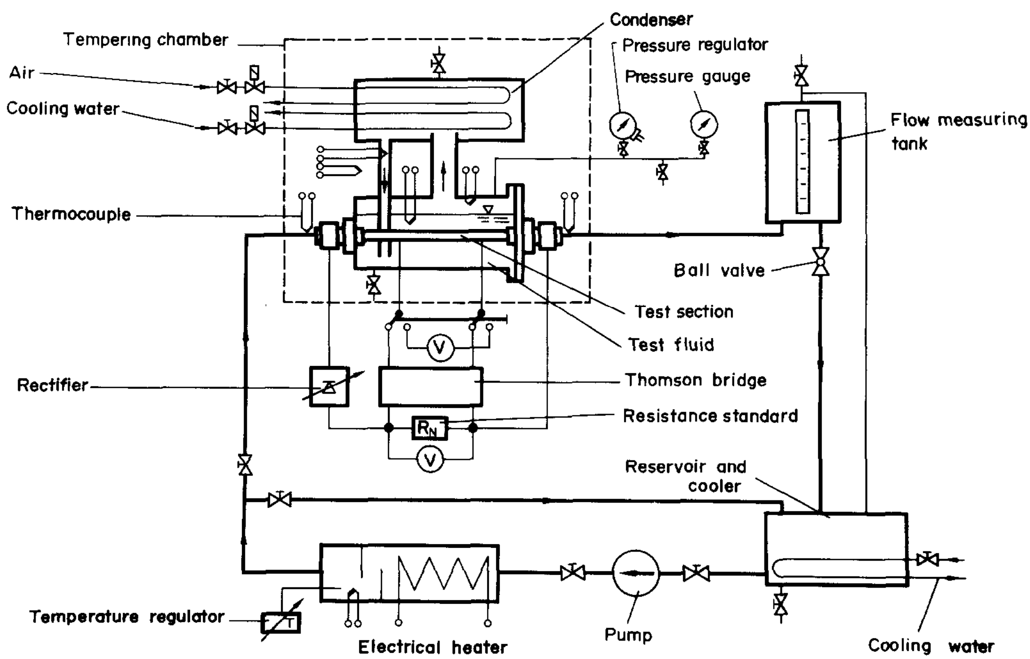

FIG. 3. Experimental equipment.

the refrigerants (Freon) R114, R12 and R113. The measurements were made at pressures between 0·5 and 30 bar. The test tubes used were a smooth and a grooved nickel tube (Fig. 4).

The measurements were to yield the average heat flux density $\dot{q}$ along the heated surface and the average temperature difference ΔT between heated surface and boiling liquid. With liquid heating the heat flux density was obtained by an enthalpy balance for the heating liquid between the two ends of the test section. The temperature difference lay between 0·6 and 1·6 K. In the case of electrical heating the heat flux density was determined by current and voltage measurements. The surface temperature could be calculated from the average wall temperature. The average wall temperature itself was obtained by measuring the electrical resistance of the test section. A disturbing factor was that this electrical resistance does not only vary with temperature but is further influenced by mechanical stresses. The influences due to mechanical stresses were taken into account in the evaluation since otherwise the results for small temperature differences ΔT would have been affected with unduly high errors (for more details on this see [16]).

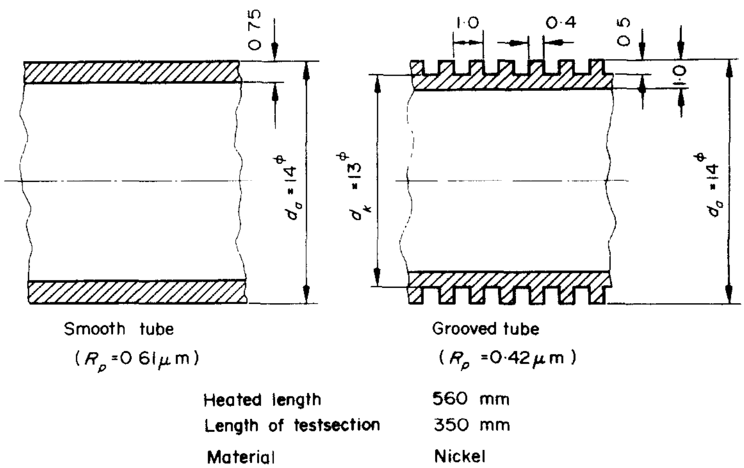

FIG. 4. Test tubes.

5. RESULTS

The results discussed in the following were all obtained with indirect heating. The results for direct electrical heating, with and without a stabilizing liquid flow, will be presented in a later paper.

5.1 *Smooth tube*

Figure 5 shows the characteristic boiling curve for R114 at a pressure of 3 bar. The measurements were repeated several times in order to verify the reproducibility. One can see that the values of the heat flux density, determined over a period of 17 days, scatter by averagely less than 5 per cent around the solid curve. The heat flux densities measured one month later, however, lie at considerably smaller temperature differences. During the time between these differing measurements all other experiments with R114 were performed, with pressures increased up to 20 bar. It seems possible that during this period, particularly due to the high boiling temperatures, there occured changes in the heating surface affecting the wettability or the nucleus formation [7]. A visible change could not be detected. Figure 6 is a joint presentation of six characteristic boiling

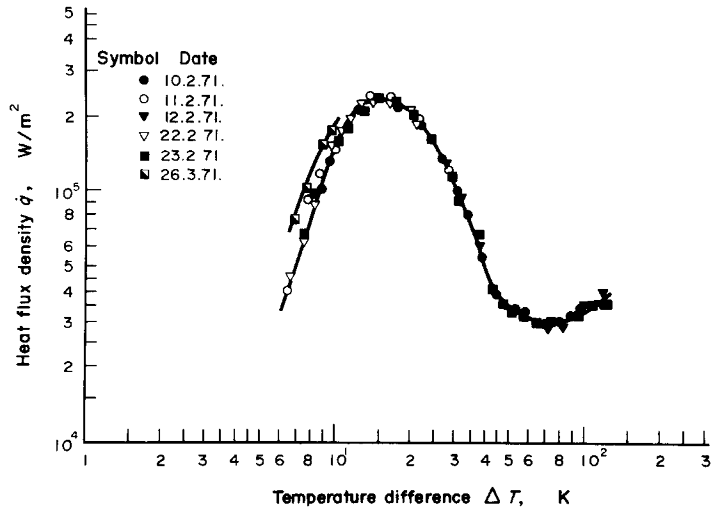

FIG. 5. Characteristic boiling curve for R114, $p = 3$ bar.

curves for R114 at pressures between 3 and 20 bar. Since the curves partly lie very close to each other, the measured points are not shown in the diagram. The experimental data are listed in Table 1. The presentation of Fig. 6 demonstrates the improvement of heat transfer to be expected in nucleate boiling with increasing pressure. The influence of pressure on the maximum heat flux density, as first established by Chichelli and Bornilla [17], is clearly recognizable. The maximum value first increases with growing pressure, reaches its peak at 9 bar and then decreases again at higher pressures. Moreover, one finds that the temperature difference ΔT at which the maximum occurs diminishes with growing pressure. The shape of the curves in the transi-

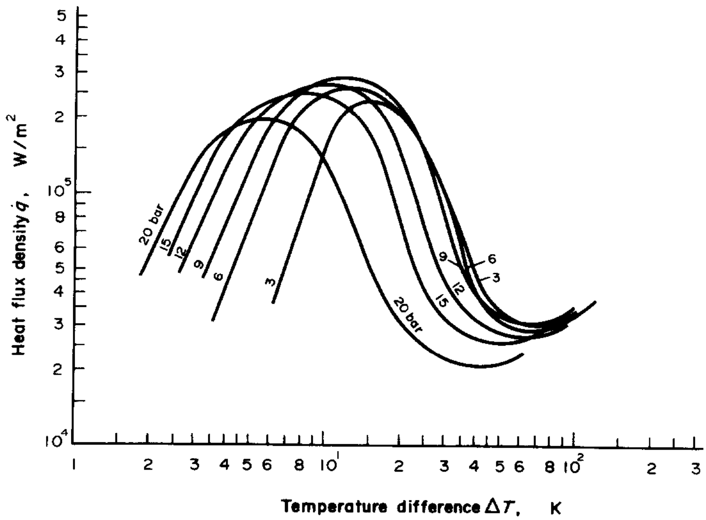

FIG. 6. Characteristic boiling curves for R114 p = 3–20 bar.

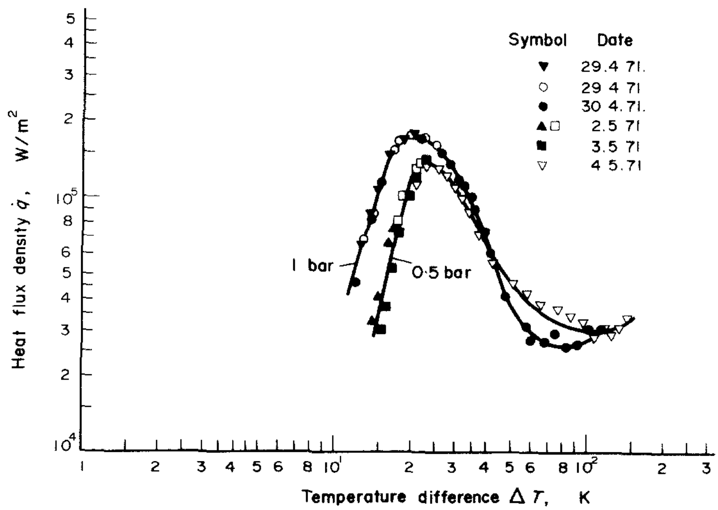

FIG. 7. Characteristic boiling curves for R113, p = 0·5–1 bar.

tion region may at first sight lead to the conclusion that the slope remained roughly the same at all pressures. This impression, however, as will be discussed later, arises only due to the logarithmic scale. We further notice in Fig. 6 that the characteristic boiling curves apparently converge in the region of film boiling. This would mean that heat transfer in film boiling is independent of pressure. The bibliography does not give us clear information concerning the pressure influence in film boiling. Both, such data that indicate an influence of pressure [18, 19] and such independent of pressure [20, 21], are to be found. Possibly the critical pressure ratio is the governing factor [22].

For R113 the characteristic boiling curves were determined at 0·5 and 1 bar (Fig. 7). As we know, this substance is less stable against thermal decomposition than, for example, R114 or R12. Therefore one soon finds deposits on the heating surface which cause a decrease in heat transfer. For this reason the measurements with R113 were performed within a shorter period and only at low boiling temperatures. Yet, it can clearly be seen from the measured data that the temperature differences grew during the repeated tests and, accordingly, heat transfer became worse. After these tests the heating surface was covered with a thin grey coating.

The tests with R12 at pressures of 7, 14 and 30 bar are shown in Fig. 8. A peculiarity in comparison with the other tests occurred at a pressure of 30 bar. At this pressure it was no longer possible to obtain steady-state operating points in the transition region. After exceeding the point of maximum heat flux density there occurred a sudden transition to a point near the minimum heat flux density. A similarly abrupt transition was recorded in the opposite direction from film boiling to nucleate boiling. Obviously the stability condition was not fulfilled. In order to verify this, the characteristic boiling curves for R12 were plotted in Fig. 9 with a linear scale. For a given heat flux density the characteristics of the heating surface were calculated by equations (1) and (3) for the conditions of the experimental apparatus and were made to intersect with the characteristic boiling curves in Fig. 9. One can now see that at pressures of 7 and 14 bar stable operating conditions are possible because the characteristics of the heating surface are steeper than the characteristic boiling curves. The flow velocities of the water inside the tube were 5 and 20 m/s. At 30 bar, however, the characteristic boiling curve in the transition

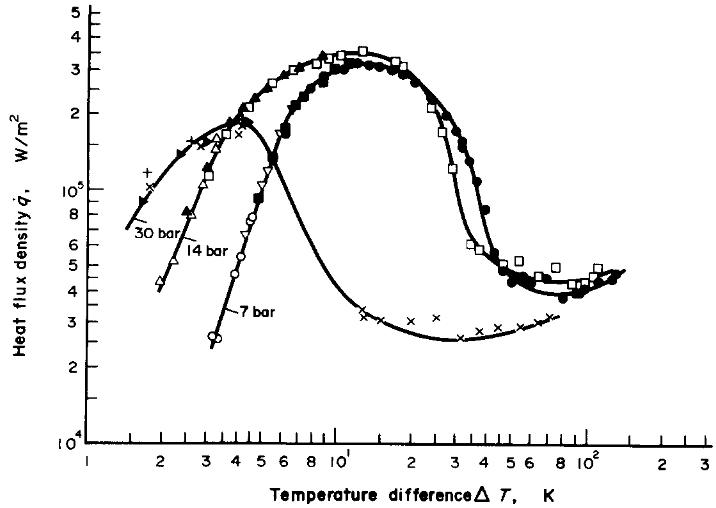

FIG. 8. Characteristic boiling curves for R12, p = 7–30 bar.

region is steeper than the characteristic of the heating surface; consequently there are no stable operating points. The statement made by the stability condition therefore corresponds to the observations in the experiment.

The diagram with the linear scale also demonstrates that the characteristic boiling curves in the transition region become steeper with increasing pressure. Stable boiling conditions in this region are therefore more difficult to achieve at high pressures than at low pressures.

5.2 *Grooved tube*

Figures 10 and 11 show the results for a grooved tube when boiling R114 at pressures of 3 and 6 bar. Curves 1 and 2 for the grooved tube present the same measurements. They only differ in the choice of the reference area for the heat flux density and the wall temperature. In the case of curves 1 the reference area for the heat flux density $\dot{q}$ is that of a smooth tube with the same outside diameter d_a, i.e. the increase in surface area due to the grooves was not taken into con-

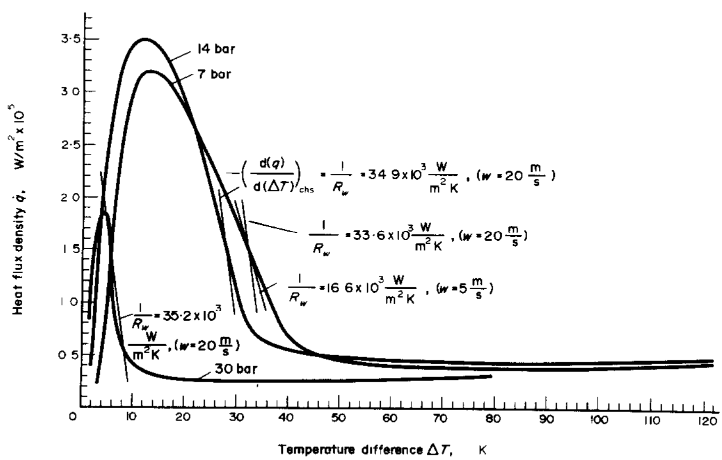

FIG. 9. Characteristic boiling curves for R12, p = 7–30 bar (linear scale).

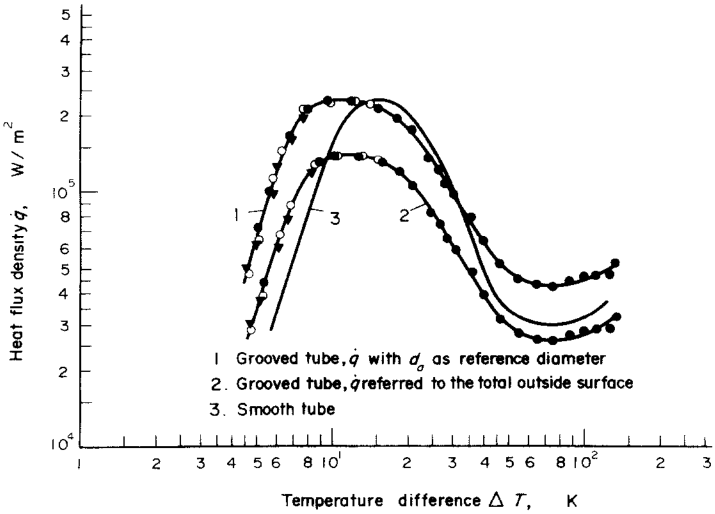

FIG. 10. Characteristic boiling curves for R114. grooved tube, $p = 3$ bar.

sideration. The wall temperature T_W is also referred to the diameter d_a. In case of curves 2 the heat flux density is referred to the total outer surface, and the wall temperature to the tube diameter at the base of the grooves. For comparison the curves 3 show heat flux densities of a smooth tube.

By comparing curves 1 and 3, one finds that, with the same outside tube diameter, heat transfer in nucleate boiling is considerably improved by grooving the tube. If one compares curves 2 and 3, one is surprises at first glance to find that in the region of nucleate boiling heat transfer from the grooved tube at a pressure of 3 bar is better than from the smooth tube, whereas it is about the same at a pressure of 6 bar.

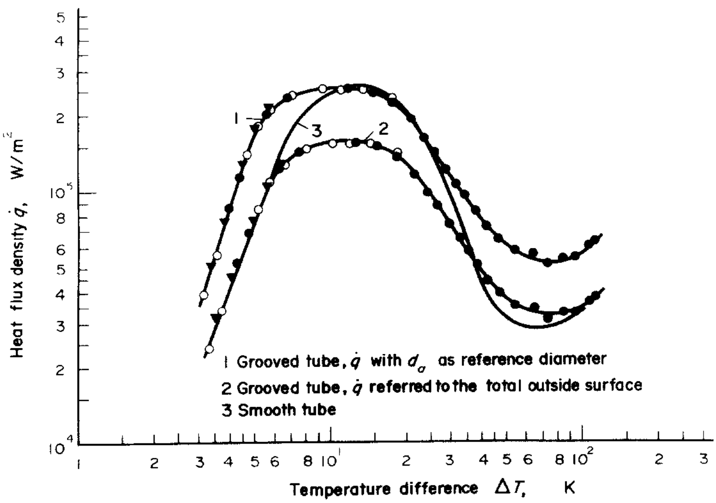

FIG. 11. Characteristic boiling curves for R114, grooved tube, $p = 6$ bar.

This behaviour is partly in accordance with observations by Gorenflo [23], who determined the heat transfer from finned tubes of various dimensions to boiling R11. Gorenflo found that, with a clearance between the fins equal to twice the bubble diameter at departure, heat transfer is lower than with tubes having either smaller or a larger clearance between the fins. He ascribed the improvement of heat transfer at larger clearance to the more favourable flow conditions between the fins. The improvement at smaller clearance is assumed to be caused by the influence of the growing bubbles on the boundary layer on both sides of the fins.

The test tube for the measurements shown in Figs. 10 and 11 had a clearance of 0·6 mm between the fins. The bubble diameter at departure [24]

$$D = 0{\cdot}01460\,\theta \sqrt{\left[\frac{2\sigma}{g(\rho_L - \rho_V)}\right]} \tag{6}$$

results, with $\theta = 35°$ [25], to 0·58 mm at 6 bar and to 0·65 mm at 3 bar. Consequently, at a pressure of 3 bar a bubble, before it departs from the surface, penetrates to the surface of the opposite fin and completely disrupts its boundary layer. This process certainly produces a considerably better heat transfer than if a bubble with smaller diameter is not able to break through the opposite boundary layer. Although the bubbles at departure do not have a fixed diameter and although equation (6) is only valid for a bubble in static equilibrium, whereas actual bubble diameters at departure vary by a distribution law, the above statement certainly remains valid since at a pressure of 3 bar more bubbles with a diameter of over 0·6 mm are formed than at a pressure of 6 bar. Gorenflo's measurements in the region of nucleate boiling always showed a higher heat transfer for finned tubes (relative to the total outer surface) than for the smooth tube, which Gorenflo attributed to additional convective influences around the finned tubes. Contrary to this, Fig. 11 shows no difference between the two tubes at a pressure of 6 bar. It may be assumed that in this case, on account of the very small clearance between the fins, the supply of liquid to the heated surface is blocked by the vapour flowing off, so that additional convection does not become effective.

According to the Figs. 10 and 11 the maximum heat flux density is approximately the same for the grooved tube and for the smooth tube (curves 1 and 3). The increase in surface area due to the grooves has no influence because the supply of liquid into the narrow grooves is disturbed by the vapour. This result is in good accordance with the tests by Burck and coworkers [26], who determined the influence of surface roughness on the maximum heat flux density in flowing water. The largest peak-to-valley height in the test was 0·3 mm. The authors established that at low velocities the maximum heat flux densities did not differ from that of a smooth tube. Bondurant and Westwater [27] on the other hand, found that the maximum heat flux density of finned tubes, depending on the dimensions of the fins, may be up to almost twice as large, as that of a smooth tube with the same outside diameter. The size of the fins and the clearance between them were, however, much greater in those experiments than with the grooved tube investigated here. These fins also permitted all three modes of boiling, i.e. nucleate boiling, transition boiling and film boiling, to be present on the fins at the same time. The authors point out that a reduction of the clearance between the fins will only cause an increase in the maximum heat flux density as long as the boiling processes do not influence each other and that a further reduction of the clearance finally has to lead to the results for a smooth tube. With respect to stable boiling conditions at maximum heat flux density and in the transition region, the most important result of the work by Bondurant and Westwater and of the present investigation is that the shape of the characteristic boiling curve can be positively influenced if the surface is equipped with fins or grooves. By such means the peak of the curve can be broadend over a larger range of the temperature difference ΔT and in the transition region it is flatter than the curve for the smooth tube. As measurements by Berenson [8] and Nishikawa and coworkers [10] show, the shape of the characteristic boiling curve can be influenced in the same way if the surface is oxidized or contaminated or if a surface-active agent is added to the boiling liquid.

6. OBSERVATIONS OF THE BOILING PROCESS IN THE TRANSITION REGION

On account of photographs Westwater and Santangelo [28] came to the conclusion that in the transition region there is no contact between the heating surface and the boiling liquid. On the other hand Berenson [8] could show with his experiments that there is in fact temporary contact between heating surface and liquid. Berenson described the boiling process in the transition region as a combination of unstable nucleate boiling and unstable film boiling with both boiling mechanisms existing alternatively at every point of the heating surface. The same results were obtained by Stock [29], who also performed measurements in the transition region. Kesselring *et al.* [11] and Nishikawa *et al.* [10] experimentally determined the temperature fluctuations on the heating surface at all points of the characteristic boiling curve. They found that the greatest temperature fluctuations occur in the upper half of the transition region near the point of maximum heat flux density. These temperature fluctuations are explained by the short contact between heating surface and liquid. With rising temperature of the heating surface the temperature fluctuation become smaller and finally disappear even before the point of minimum heat flux density is reached [11]. Accordingly in the lower part of the transition region the liquid no longer touches the heating surface. Observations of the author and photographs of the boiling process also indicate that already before reaching the point of minimum heat flux density there exists on the heating surface a continuous vapour film that is no longer broken by the liquid. The liquid–vapour interface, however, is still in vigorous motion, which can be recognized from the ragged lines of reflected light in Fig. 12. On the other hand, in the region of film boiling an almost smooth interface can be observed (Fig. 13).

REFERENCES

1. K. STEPHAN, Stabilität beim Sieden, *Brennst.—Wärme—Kraft* **17**(12), 571–578 (1965).
2. K. STEPHAN, Ubertragung hoher Wärmestromdichten an siedenee Flüssigkeiten, *Chemie-Ingr. Tech.* **38**(2), 112–117 (1966).
3. S. A. KOVALEV, On methods of studying heat transfer in transient boiling, *Int. J. Heat Mass Transfer* **11**(2), 279–283 (1968).
4. P. GRASSMANN and H. ZIEGLER, Zur Stabiltät von Strömungen in geschlossenen Kreisen, *Chemie-Ingr.-Tech.* **41**(16), 908–915 (1969).
5. L. A. HALE and G. B. WALLIS, Thermal stability of surfaces heated by convection and cooled by boiling, *I/EC Fundamentals* **11**(1), 46–52 (1972).
6. S. A. KOVALEV, V. M. ZHUKOV, G. M. KAZAKOV and YU. A. KUZMA-KICHTA, Effect of coating with low thermal conductivity upon boiling heat transfer of liquid on isothermal and non-isothermal surfaces, *Fourth Int. Heat Transfer Conf. Paris* B 1.4 (1970).
7. D. R. VERES and L. W. FLORSCHUETZ, A comparison of transient and steady-state pool-boiling data obtained using the same heating surface, *J. Heat Transfer* **93C**(2), 229–232 (1971).
8. P. J. BERENSON, Experiments on pool-boiling heat transfer, *Int. J. Heat Mass Transfer* **5**, 985–999 (1962).
9. F. D. MOORE and R. B. MESLER, The measurement of rapid surface temperature fluctuations during nucleate boiling of water, *A.I.Ch.E. Jl* **7**(4), 620–624 (1961).
10. K. NISHIKAWA, S. HASEGAWA and H. HONDA, Studies on boiling characteristic curve, *Mem. Fac. Engng Kyushu Univ.* **27**, 133–154 (1967).
11. R. C. KESSELRING, P. H. ROCHE and S. G. BANKOFF, Transition and film boiling from horizontal strips, *A.I.Ch.E. Jl* **13**(4), 669–675 (1967).
12. S. A. KOVALEV, On methods of studying heat transfer in transient boiling, *Int. J. Heat Mass Transfer* **13**, 1505–1506 (1970).
13. K. STEPHAN, On methods of studying heat transfer in transient boiling, *Int. J. Heat Mass Transfer* **11**, 1735–1736 (1968).
14. H. J. VAN OUWERKERK, Burnout in pool boiling the stability of boiling mechanisms, *Int. J. Heat Mass Transfer* **15**, 25–34 (1972).
15. P. G. POLETAVKIN, V. J. PETROV, L. D. DODONOV and J. T. ALADIEV, A new method of investigation of boiling heat transfer, *Dokl. Akad. Nauk SSSR* **40**(5), 775–776 (1953).
16. G. HESSE, Wärmeübergang bei Blasenverdampfung, bei maximaler Wärmestromdichte und im Übergangsbereich zur Filmverdampfung, Diss., Techn. Universität Berlin (1972).

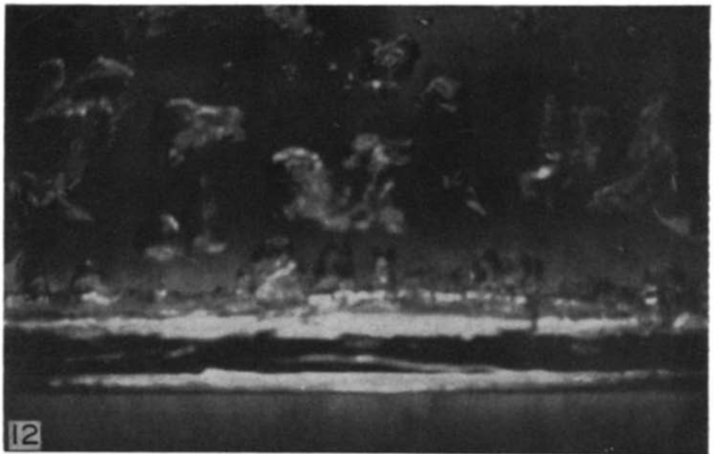

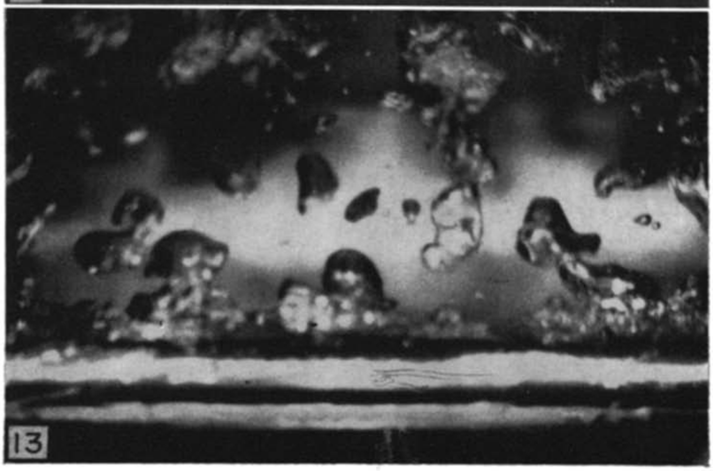

FIG. 12. Transition boiling, R113, $p = 1$ bar, $\dot{q} = 30\,000$ W/m^2, $\Delta T = 61$ K.

FIG. 13. Film boiling, R113, $p = 1$ bar, $\dot{q} = 28\,000$ W/m^2, $\Delta T = 104$ K.

17. M. T. Cichelli and C. F. Bonilla, Heat transfer to liquids boiling under pressure, *Trans. Am. Inst. Chem. Engrs* **41**, 755–787 (1945).
18. P. Pitschmann and U. Grigull, Filmverdampfung an waagerechten Zylindern, *Wärme- und Stoffübertragung* **3**, 75–84 (1970).
19. R. D. Wright, L. D. Clements and C. P. Colver, Nucleate and film pool boiling of ethane–ethylene mixtures, *A.I.Ch.E. Jl* **17**(3), 626–630 (1971).
20. U. Grigull and E. Abadzic, Heat transfer from a wire in the critical region, *Proc. Instn. Mech. Engrs* 182(31), 52–57 (1967–68).
21. E. Abadzic and R. J. Goldstein, Film boiling and free convection heat transfer to carbon dioxide near the critical state, *Int. J. Heat Mass Transfer* **13**, 1163–1175 (1970).
22. R. J. Simoneau and K. J. Baumeister, Experimental effects of pressure, subcooling, and diameter on thin-wire film boiling of liquid nitrogen, *Adv. Cryogenic Engng* **16**, 416–425 (1971).
23. D. Gorenflo, Zum Wärmeübergang bei der Blasenverdampfung an Rippenrohren, Diss. T.H. Karlsruhe (1966).
24. W. Fritz, Berechnung des Maximalvolumes von Dampfblasen, *Phys. Z.* **36**, 379–384 (1935).
25. K. Stephan, *Beitrag zur Thermodynamik des Wärmeübergangs beim Sieden*. Abhandl. des Deutsch. Kältetechn. Vereins Nr. 18. C. F. Müller, Karsruhe (1964).
26. E. Burck, W. Hufschmidt and E. de Clercq, Einfluss künstlicher Rauhigkeiten auf die kritische Wärmestromdichte bei erzwungener Konvektion, *Atomkernenergie* **14**(5), 305–308 (1969).
27. D. L. Bondurant and J. W. Westwater, Performance of transverse fins for boiling heat transfer, *Chem. Engng Prog. Symp. Ser.* **67**(113), 30–37 (1971).
28. J. W. Westwater and J. G. Santangelo, Photographic study of boiling, *Ind. Engng Chem.* **47**, 1605–1610 (1955).
29. B. J. Stock, Observations on transition boiling heat transfer phenomena, ANL-6175 (1960).

APPENDIX

Table 1. R114 test data

Date	$\dot{q}$ [W/m^2]	ΔT [K]	$\Delta h/h$ [%]
$p = 3$ bar			
22 Feb. 1971	46 600	6·68	12·9
	62 700	7·60	9·8
	87 900	8·37	7·2
	150 500	9.93	8.3
	174 900	10·76	7.2
	197 300	11·62	6·5
	216 600	12·74	7·2
	231 200	14·31	6·7
	231 200	16·60	6·6
	211 300	20·08	7·2

Table 1—continued

$p = 3$ bar			
	191 300	21·81	7·9
23 Feb.	67 000	7·44	9·9
	159 600	10·08	8·5
	177 200	10·95	7·4
	212 900	12·81	6·3
	233 500	14·80	5·7
	224 600	17·10	5·8
	199 600	20·70	6·4
	162 200	24·50	7·7
	116 400	29·20	10·6
	92 500	32·50	7·2
	68 200	38·05	9·5
	40 700	43·10	9·4
	35 800	47·40	10·5
	33 100	52·00	10·4
	32 050	57·90	10·5
	30 600	64·80	14·3
	30 700	73·60	13·9
	29 400	84·20	13·8
	32 500	96·30	14·3
	36 700	108·90	14·7
	36 800	123·20	14·7
26 Feb.	77 900	6·92	10·8
	103 700	7·62	8·6
	155 900	8·98	8·6
	175 700	9·70	7·6
$p = 6$ bar			
5 March	108 100	5·64	9·5
	169 700	6·89	8·3
	216 000	8·24	6·7
	258 000	10·30	6·3
	267 400	13·40	5·9
	243 300	17·35	6·2
	200 900	20·57	5·8
	146 200	25·45	7·7
	93 000	32·16	11·6
	68 400	35·60	7·2
	39 300	42·65	14·7
	30 500	70·80	13·3
	31 900	82·30	12·6
	33 800	93·90	12·3
	36 400	104·50	11·6
6 March	73 900	4·59	12·2
	90 900	5·57	10·9
	111 400	6·00	8·5
	153 100	6·72	8·6
	189 900	7·55	7·9

Table 1—continued

$p = 9$ bar			
9 March	57 200	3·53	10·0
	86 900	4·43	9·8
	123 400	4·78	9·8
	170 500	5·75	9·4
10 March	90 100	4·64	11·4
	155 900	5·62	9·2
	190 500	6·24	7·9
	230 700	7·50	7·8
	254 600	8·61	7·0
	280 900	10·60	6·5
	288 700	12·52	5·8
	270 700	15·97	5·9
	154 200	24·31	9·7
	148 500	25·10	7·4
	112 900	27·98	11·8
	75 900	30·90	14·9
	56 900	33·60	12·3
	47 400	35·60	15·6
	37 700	41·70	13·3
	30 300	63·20	13·0
	30 800	73·70	12·6
	31 600	84·10	12·3
	35 000	91·30	11·5
	35 400	94·70	11·3
$p = 12$ bar			
14 March	78 000	3·34	12·9
	97 700	3·66	11·1
	147 300	4·31	10·3
	173 300	4·73	9·1
	202 000	5·43	9·1
16 March	145 100	4·23	11·0
	168 500	4·85	9·5
	195 900	5·49	9·2
	213 100	5·99	8·9
	242 700	7·09	8·1
	252 700	7·91	7·6
	273 300	9·65	6·9
	271 000	11·46	6·7
	242 900	14·93	7·1
	137 400	20·32	14·7
	87 500	24·93	16·9
	55 800	28·18	15·8
	42 500	31·85	16·4
	38 900	37·15	17·5
	28 600	65·53	16·6
	27 200	74·80	16·9
	34 000	84·80	14·7
$p = 15$ bar			
19 March	88 400	2·77	15·5
	142 500	3·85	13·9
	166 700	3·95	12·5
	213 900	5·20	12·2
	233 600	6·04	10·1
	246 500	7·23	9·2
	246 200	9·90	8·8
	220 600	11·69	9·5
	139 000	16·81	14·4
	126 200	17·31	15·7
	87 800	19·12	21·8
	53 700	22·36	22·7
	46 800	23·98	15·2
	32 400	28·84	11·4
	30 400	32·68	11·8
	26 500	65·59	14·9
	28 300	73·83	14·5
20 March	76 400	2·76	18·6
	102 400	3·10	15·1
	148 100	3·76	13·4
	192 700	4·55	12·1
	221 500	5.28	10·6
$p = 20$ bar			
22 March	86 400	2·45	16·9
	122 800	2·91	14·3
	152 200	3·38	13·7
	181 600	4·30	13·3
	198 800	5·24	12·0
23 March	109 400	2·64	17·6
	129 900	3·13	14·9
	174 900	4·08	13·2
	191 200	4·82	10·7
	203 200	5·57	9·8
	201 000	5·65	9·9
	150 200	9·22	11·3
	195 400	5·48	10·1
	126 400	10·12	13·1
	63 800	13·97	23·9
	54 700	15·59	16·2
	33 700	17·76	23.8
	31 700	19·49	16·2
	25 300	23·83	18·5
	22 700	43.18	16·4
	20 900	49.11	16·9
	24 500	55·30	14·9

Table 2. R12 test data

date	$\dot{q}$ [W/m²]	ΔT [K]	$\Delta h/h$ [%]
p = 7 bar			
10 April	66 000	4·38	13·6
	104 400	5·06	12·1
	120 800	5·38	10·6
	169 800	6·05	10·3
	213 900	6·72	9·4
13 April	170 900	6·30	9·0
	255 300	7·95	7·9
	286 600	8·94	7·0
	304 700	10·80	6·4
	320 600	12·06	6·0
	317 700	13·59	5·9
	316 800	14·94	5·9
	305 900	16·71	6·0
	295 300	18·45	6·2
	273 900	20·48	6·5
	239 300	24·34	7·4
	202 400	27·31	8·6
	173 100	29·66	10·0
	152 200	32·17	11·3
	133 700	34·68	7·6
	110 200	36·68	9·1
	85 500	40·34	11·6
	57 500	43·72	11·1
	49 600	46·39	8·1
	43 900	51·11	8·5
	46 300	52·93	9·7
	38 400	83·72	13·5
	41 200	102·55	12·6
	44 300	115·0	11·2
	47 900	133·24	10·0
p = 14 bar			
19 April	44 800	1·98	19·6
	53 300	2·24	17·2
	82 200	2·62	16·6
	108 300	2·95	14·1
	161 900	3·31	12·1
	150 800	3·34	11·9
20 April	113 000	3·08	15·5
	167 600	3·61	11·7
	216 600	4·37	10·0
	269 400	5·55	8·5
	301 400	6·69	7·6
	320 900	8·33	7·1
	339 600	9·22	6·2
	348 500	10·44	5·9
	356 000	12·77	5·5
	324 200	17·30	5·7
	310 800	18·40	5·9
	214 600	24·05	8·3
	171 700	26·60	10·2
	123 700	29·11	13·8

Table 2—continued

p = 14 bar			
20 April	61 600	35·16	13·8
	58 500	37·60	10·3
	50 800	47·18	13·7
	46 500	65·53	13·5
	42 700	88·70	13·5
	42 800	100·05	13·0
	46 300	107·10	12·2
p = 30 bar			
22 April	91 400	1·70	20·3
	136 200	2·41	16·5
	155 200	2·60	15·0
	156 600	3·10	13·6
	185 200	4·37	11·3
23 April	103 100	1·81	19·7
	147 400	2·83	14·5
	180 500	4·21	10·8
	33 800	12·67	21·7
	31 100	12·97	22·9
	30 700	15·06	17·5
	30 200	20·10	17·2
	25 900	31·84	14·7
	27 800	37·60	13·7
	28 400	45·03	13·1
	28 700	55·10	12·5
	29 800	64·20	12·0
	31 300	71·30	11·5

Table 3. R113 test data

Date	$\dot{q}$ [W/cm²]	ΔT [K]	$\Delta h/h$ [%]
p = 1 bar			
29 April	66 400	12·65	14·0
	86 800	13·74	10·9
	107 200	14·79	8·9
	148 400	16·85	10·7
	170 800	19·14	9·3
	178 100	20·79	8·9
30 April	47 000	12·21	14·5
	86 000	14·18	13·7
	116 300	15·47	10·3
	173 000	19·70	9·6
	174 800	22·54	9·5
	154 100	26·90	10·6
	120 000	31·10	13·3
	112 600	33·10	14·3

Table 3—*continued*

p = 1 bar			
30 April	102 900	35·20	9·5
	90 600	36·10	10·6
	74 900	39·20	12·7
	61 600	42·10	10·9
	54 500	45·10	12·1
	41 800	48·00	13·3
	31 400	58·20	16·1
	27 500	60·50	18·5
	27 300	69·10	13·7
	29 100	75·60	13·3
	26 100	84·40	13·0
	26 200	93·30	12·5
	31 300	102·80	10·7
	30 900	116·60	12·6
p = 0·5 bar			
2 May	81 600	17·59	11·7
	101 100	18·82	9·6
	127 700	21·19	12·0
	137 300	22·82	11·2
	76 400	17·67	11·9
	67 000	16·86	13·6
	40 900	15·34	12·6
	33 000	14·45	15·5
3 May	139 200	23·60	10·7
	120 900	21·65	12·4
	102 700	20·06	14·3
p = 0·5 bar			
	73 400	18·28	9·8
	52 400	17·21	13·4
	37 600	16·27	12·8
	30 100	15·46	15·8
4 May	116 500	20·18	9·4
	137 700	23·12	12·2
	132 480	25·51	12·7
	124 700	28·21	13·4
	108 900	30·80	15·1
	100 300	32·50	10·4
	89 200	34·70	11·6
	71 800	37·90	13·8
	66 500	40·60	15·1
	55 300	43·80	9·2
	46 100	53·10	11·1
	42 100	59·80	11·6
	37 600	66·80	12·3
	36 700	78·60	12·0
	34 800	88·00	12·2
	32 300	99·60	12·2
	28 400	108·80	14·9
	30 400	119·40	14·9
	28 100	130·10	14·3
	30 300	139·10	13·0
	33 800	149·50	12·3

TRANSFERT THERMIQUE EN EBULLITION NUCLEEE, FLUX THERMIQUE MAXIMAL ET EBULLITION DE TRANSITION

Résumé—Des courbes caractéristiques de l'ébullition de réfrigérants (Fréon) R12, R113 et R114 ont été déterminées à des pression jusqu'à 30 bar. Les fluides étudiés bouillaient sur la face externe d'une tube lisse de nickel et d'un tube rainuré.

Par application de la condition de stabilité de Stéphan, des points stables de fonctionnement ont pu être maintenus à une densité maximale de flux thermique et dans la région de transition. Due aux pentes différentes des courbes caractéristiques d'ébullition, la condition de stabilité dans la région de transition est plus facile à réaliser à des pressions faibles qu'à de hautes pressions. Par utilisation d'un tube d'essai rainuré, il a été possible d'influencer favorablement la forme des courbes caractéristiques d'ébullition relativement au transfert thermique et à la stabilité.

WÄRMEÜBERGANG BEI BLASENVERDAMPFUNG, MAXIMALER WÄRMESTROMDICHTE UND IM ÜBERGANGSBEREICH ZUR FILMVERDAMPFUNG

Zusammenfassung—Siedekennlinien der Kältemittel (Freon) R12, R113 und R114 wurden für Drücke bis zu 30 bar emittelt. Die Flüssigkeiten verdampften an der Aussenseite eines glatten und eines mit Rillen versehenen Rohres aus Nickel.

Unter Berücksichtigung der Stabilitätsbedingung von Stephan konnten bei maximaler Wärmestromdichte und im Übergangsbereich stabile Betriebspunkte eingestellt werden. Wegen der unterschiedlichen Steigung der Siedekennlinien ist die Stabilitätsbedingung im Übergangsbereich bei niedrigem Druck leichter einzuhalten als bei hohem Druck. Durch die am Verdampferrohr angebrachten Rillen konnte die Form der Siedekennlinien bezüglich des Wärmeüberganges und der Stabilität güunstig beeinflusst werden.

ПЕРЕНОС ТЕПЛА В ПЕРЕХОДНОМ РЕЖИМЕ ЯДЕРНОГО КИПЕНИЯ В УСЛОВИЯХ МАКСИМАЛЬНОГО ТЕПЛОВОГО ПОТОКА

Аннотация—Определялись характеристические кривые кипения охладителей (фреона) $R12$, $R113$ и $R114$ при давлениях до 30 бар. Процесс кипения жидкости происходт на внешней стороне гладкой никелевой трубы и трубы с канавками. Применяя условие устойчивости Стефана, можно получить устойвые рабочие точки для максимальной плотности теплового потока и для переходной области. Благодаря различию в наклонах характеристических кривых кипения условие устойчивости в переходной области легче выполнимо при низких давлениях, нежели при высоких. Используя экспериментальную трубку с канавками, можно влиятв на форму характериситческой кривой кипения в отношении переноса тепла и устойчивости.